ORIGINAL RESEARCH PAPER

Spectroscopic studies on the interaction of Fe$_3$O$_4$@CaAl LDH@ Lamivudine with the calf thymus DNA

Nahid Shahabadi[1],*, Mahtab Razlansari[1] and Avat (Arman) Taherpour[2]

[1] *Inorganic Chemistry Department, Faculty of Chemistry, Razi University, Kermanshah, Iran*
[2] *Organic Chemistry Department, Faculty of Chemistry, Razi University, Kermanshah, Iran*

ABSTRACT

In this study, we were synthesized Fe$_3$O$_4$@LDH@Lamivudine and characterized by FT-IR spectroscopy, XRD and TEM. The interaction of this nanoparticle with CT-DNA was investigated by viscosity, circular dichroism (CD), Uv-Visible and fluorescence spectroscopy. Among all nanocarriers which applied as drug delivery vectors, layered double hydroxides (LDHs) with exchangeable anions in the positive brucite-like interlayers have been attracting much attentions in the field of cellular delivery of anionic drug and other bio-functional molecules, due to their low toxicity, biocompatibility, high stability, pH dependent solubility and enhanced cellular uptake behavior compared with the conventional drug carriers. UV-Visible absorption studies indicated hyperchromism with the binding constant of 4.9×10^3 M^{-1}. In the fluorimetric investigation, this nanocomposite can bind to DNA and creates a new non-fluorescence adduct. The thermodynamic parameters (ΔH<0 and ΔS<0), indicate that the interaction between DNA and nanocomposite is hydrogen bond and Vander-Waals force. The process of binding was spontaneous, in which Gibbs free energy change (ΔG) was negative. Furthermore, viscosity measurements did not show any changes by increasing the amount of the mentioned nanocomposite. In Circular dichroism, both positive and negative bands illustrate little changes, which imply a non-intercalative mode of binding. The experimental results demonstrated that Fe$_3$O$_4$@LDH@Lamivudine interact with DNA by groove binding mode. As an evidenced, increasing the fluorescence intensity of Hoechst–DNA solutions in the presence of different amounts of Fe$_3$O$_4$@LDH@Lamivudine nanoparticles are able to displace the Hoechst molecules, which was grooved into DNA completely as to indicate groove binding mode.

Keywords: *CT-DNA; Fe$_3$O$_4$; Groove Binding; Lamivudine; Layered Double Hydroxide*
© 2018 Published by Journal of Nanoanalysis.

INTRODUCTION

Many antiviral, anticancer, antibiotic drugs demonstrate their initial biological effects from interaction with Deoxyribonucleic acid (DNA). Hence, these biomacromolecules illustrate the main purpose of drug progress strategies designed to develop next-generation therapeutics for illness such as cancer [1]. Cancer is an important cause of death around the world, each year many people die because they can't receive appropriate treatment, chemotherapy is expensive and few people can afford it, so finding a new and inexpensive drug with both anticancer effects and saving its own properties can be a good way to treat cancers easily in future [2]. First of all, we need to investigate their interaction with biomacromolecules such as DNA. DNA is the most important part of the cell component that carries on genetical information and mostly is a target for tiny molecules like drug-nanocarriers. Such nanocomposites display DNA-targeted pharmacological functions as they disturb DNA replication, the primary phase of cell division and cell growth. They can also interfere with the synthesis of protein transcription processes [3].

* Corresponding Author Email: *nahidshahabadi@yahoo.com*

Nowadays the use of magnetic nanoparticles (MNPs) in medical applications has exceeded expectations [4]. Small size and vast surface area of MNPs can cause the aggregation of nanoparticles. So coating the surface of magnetic cores by surface engineering is an important step in synthesis new nanoparticles for drug carrying systems. Fe_3O_4 nanoparticles as core structure can be coated by various inorganic or organic shell substances, which developed to enhance the effect of NPs on drug loading and keep them versus aggregation and induction the new attributes to the nanoparticles e.g. catalytic properties, biological diagnosis applications, thermo responsiveness. In this study, in order to protect magnetic nanoparticles from aggregation, layered double hydroxides were applied as the shell structure [5]. Layered double hydroxides (LDHs) are biocompatible 2D inorganic compound and receive great attention as drug carriers because of the widespread requirements to improve advanced drug delivery systems (DDS), that is certainly relevant to universal issues like as the well-being and health care of human being, along with extended life, and dominance of illnesses [6]. The most noteworthy feature of LDH as a drug delivery carrier is particle size dependency for cellular uptake behavior. The particle size of LDH nanoparticles smaller than ~250 nm can be transpired into cells via clathrin-mediated endocytosis [7]. Loading drug on nanoparticles can improve the effectiveness and toxicity of drugs on cancer cells and it can also save and protect the drug till achieving the target cells [8]. Lamivudine is called 3TC is an antiretroviral drug and nucleoside analog, nucleoside reverse transcriptase (RT) inhibitors [9], the main application of Lamivudine refers to prevention and treatment of HIV/AIDS [10]. In recent studies, results indicated that the binding mode of Lamivudine and CT-DNA was groove binding [11]. The main goal of this study is to determine the binding mode of Fe_3O_4@LDH@ Lamivudine with CT-DNA by spectroscopic methods.

EXPERIMENTAL AND METHODS MATERIALS

Methylene blue (MB), Hoechst 33258, Deoxyribonucleic acid sodium salt from calf thymus (CT-DNA) purchased from Sigma Aldrich company, used without any purifications. Tris-HCl, phosphate buffer saline (PBS), Iron (III) chloride hexahydrate ($FeCl_3.6H_2O$), Iron (II) Chloride tetrahydrate ($FeCl_2.4H_2O$), ammonia

(25%), Hydrogen chloride 37% (HCl), Sodium hydroxide (NaOH), Calcium Nitrate Tetrahydrate ($Ca(NO_3)_2.4H_2O$), aluminum nitrate, nonahydrate ($Al(NO_3)_3.9H_2O$), Methanol, Ethanol, sodium carbonate (Na_2CO_3) and Lamivudine, were provided and purchased from Merck Company.

Apparatus and methods

The morphology and particle size of the nanocomposites were characterized by transmission electronic microscopy (TEM, Philips, EM208, 100 kV). Powder X-ray diffraction (XRD, Rigaku, D/Max-RA, Cu Ka) was applied to recognize the crystal structure of the samples. The Fourier-transform infrared spectroscopy (FT-IR) spectra were recorded with KBr pellets using a Bruker ALPHA FT-IR spectrometer. Fluorescence measurements were carried out by JASCO spectrofluorimeter (FP6200) using a 1 cm path length of quartz cuvette. Uv-visible spectra were recorded by Agilent 8453. CD measurements were carried out by a JASCO (J-810) spectropolarimeter at 25 °C. The viscosity was measured (SCHOT AVS 450) at room temperature.

Synthesis of Fe_3O_4

The Fe_3O_4 magnetic nanoparticles were synthesis trough a co-precipitation method. In order to achieve this purpose, ferric chloride hexahydrate $FeCl_3.6H_2O$ (3.25 g) and ferrous chloride tetrahydrate $FeCl_2.4H_2O$ (1.6 g) with the molar ratio of 2Fe(III):1Fe(II) were dissolved in 250 mL of distilled water under N_2 atmosphere by vigorous stirring (60 °C). Then pH value of the solution was adjusted (pH=10), by subjoining 15 mL of 25% NaOH solution quickly and reaction was performed under continuous stirring (500 rpm) for 1 h at 60 °C. The black precipitation was cooled down to the temperature of room and washed 3 times with double distilled water and ethanol to remove unreacted chemicals. The magnetite precipitates were dried at room temperature for 24 h under vacuum [12].

Synthesis of Fe_3O_4@LDH

First of all, the slick suspension got ready by ultrasonication of Fe_3O_4 (0.3 g) into 75 mL solvent (Vmethanol/Vwater=1/1) for 20 min. In the following step, 50 mL alkaline solution of Na_2CO_3 and sodium hydroxide (NaOH) (0.16 g and 0.24 g respectively) was added dropwise into the ready suspension until pH ca. 10.0 and

hold for 10 min. Then 50 mL of the salt solution of 0.45 g of Aluminum (III) nitrate nonahydrate $(Al(NO_3)_3 \cdot 9H_2O)$, and 0.85 g of calcium (II) nitrate tetrahydrate $(Ca(NO_3)_2 \cdot 4H_2O)$ was added to the former suspension and applying the alkaline solution of Na_2CO_3 and NaOH, the pH of above mixture was adjusted to 10.0. The obtained slurry dispersion was stirred vigorously for 5 min then collected by a magnet and washed three times with deionized water and ethanol. Finally, Fe₃O₄@CaAl LDH was dried 24 h at 60 °C and the desired product was collected.

Preparing Fe₃O₄@LDH@ Lamivudine

Loading the Lamivudine into the structure and on the surface of Fe₃O₄@CaAl LDH was accomplished by appending 0.01 g of Fe₃O₄@CaAl LDH to 30 mL of 2.5 mM Lamivudine solution in distilled water and stirred for 24 h at 25 °C. In this level, the pH value of the solution adjusted to 7.4. The resulting solid was separated by applying a magnet, then washed three times with distilled water and dried under vacuum condition at 25 °C and the final product was achieved (Fe₃O₄@CaAl@ Lamivudine) [13].

DNA binding studies

In the first step, the concentration of CT-DNA was measured by UV-vis absorbance at 260 nm, then calculating the concentration of CT-DNA by using (ε_p) of 6600 $M^{-1}cm^{-1}$. ε_p is the extinction coefficient at 260 nm. The entire experiments of CT-DNA were done with Tris-HCl buffer solution (pH 7.4) at room temperature. In order to investigate the

binding mode of Fe₃O₄@CaAl@Lamivudine with CT-DNA, fluorescence and Uv-vis spectroscopy, viscosity and CD spectropolarimetry were applied [14].

RESULTS AND DISCUSSIONS
Characterization of the Fe₃O₄@LDH@Lamivudine
XRD analysis

The XRD patterns of Fe₃O₄, Fe₃O₄@CaAl LDH, and Fe₃O₄@CaAl@Lamivudine were demonstrated in Fig. 1. In the XRD pattern of Fe₃O₄ (curve a), the diffraction peaks were identified with cubic-phase Fe₃O₄ crystalline structure [JCPDS-019-0629]. The (220), (311), (400), (422), (511) and (440) reflections of typical Fe₃O₄ in 2θ = 30.2°, 35.7°, 43.1°, 53.3°, 56.8° and 62.8° affirm the great crystallinity of the Fe₃O₄ nanoparticles. The XRD pattern of Fe₃O₄@CaAl LDH obviously illustrated the formation of CaAl LDH shell around Fe₃O₄ nanoparticles (curve b). moreover, the Fe₃O₄ reflections, the diffraction pattern of resulting Fe₃O₄@CaAl LDH core-shell structure, represents specified absorption peaks at 10.1°, 20.2°, 30.6°, 37.3°, 48.2°, 62.6°, 63.1° which are ascribed to the (003), (006), (009), (015), (018), (110) and (113) facets of LDH structures [15].

The XRD pattern of Fe₃O₄@CaAl@Lamivudine nanostructure undoubtedly shows the characteristic peaks of CaAl LDH and Fe₃O₄ nanoparticles. The broadening and shift of (003) basal reflection of Fe₃O₄@CaAl LDH indicates that the Lamivudine molecules are perfectly loaded on the surface and intercalated into the layers of the Fe₃O₄@CaAl LDH structure (curve c).
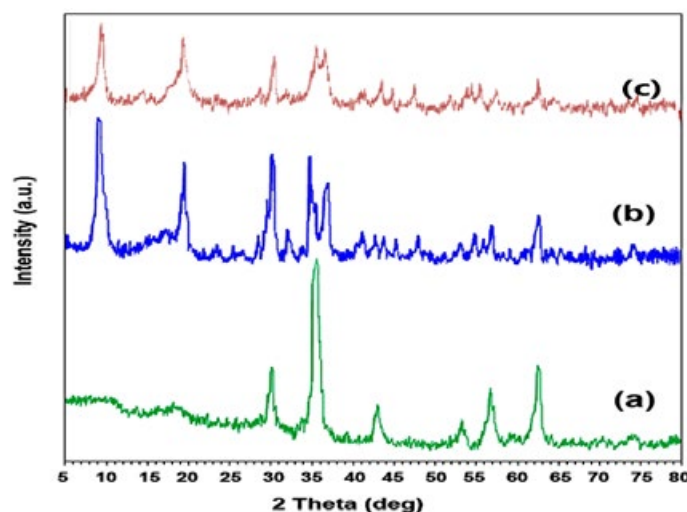

Fig. 1. XRD patterns of a) Fe₃O₄, b) Fe₃O₄@CaAl LDH and c) Fe₃O₄@CaAl@Lamivudine.

TEM analysis

Transmission electron microscopy (TEM) images obviously demonstrated MNPs. It shows the core-shell structure of Fe_3O_4@LDH and Lamivudine drug which was loaded on the surface and into the structure of nanoparticles (Fig. 2). It can be clearly perceived that nanoparticles were mostly semi-spherical with similar particle size. The particle size was averagely about 125 nm in the TEM image [16].

FT-IR analysis

The FT-IR spectra of the Lamivudine, Fe_3O_4, Fe_3O_4@CaAl-LDH, Fe_3O_4@CaAl@Lamivudine were shown in Fig. 3. Lamivudine exhibits main characteristic bands of carbonyl (C=O-NR$_2$) stretching at 1632 cm^{-1}. This band overlaps the band due to N-H bending at 1607 cm^{-1}. The band due to stretching vibration of the imine group (R$_2$-C=NR) is observed at 1648 cm^{-1}. Broad bands due to the stretching vibration of -NH$_2$ and -OH group are observed at 3300-3500 cm^{-1} [17, 18]. The absorption peaks at 568 cm^{-1} belonged to the stretching vibration mode of Fe-O bonds in Fe_3O_4. The FT-IR spectrum of Fe_3O_4@CaAl LDH, in addition to Fe_3O_4 absorption bands which the Fe-O vibrations of magnetite phase absorption bands at about 575 cm^{-1} were observed and shows the bands at 496 and 521 cm^{-1} that are related to the M-O vibration modes of CaAl-LDH structure (curve c). It is notable that the characteristic absorption band around 1388 cm^{-1} is related to the presence of CO_3^{2-} in the LDH structure [19]. NPs exhibit a strong band due to stretching mode of the -OH group at 3,400
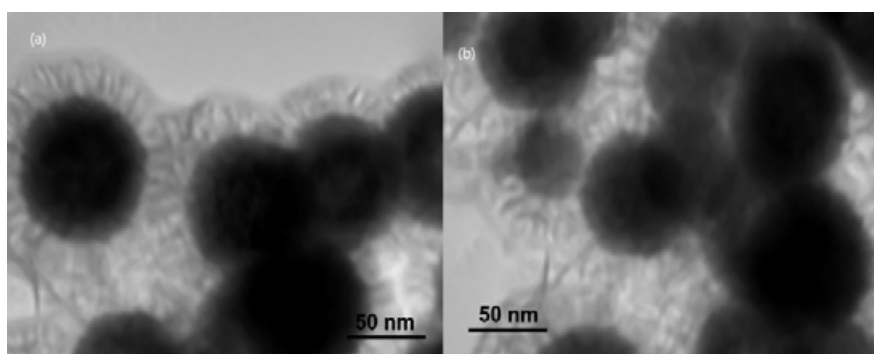

Fig. 2. TEM images of a) high magnification and b) low magnification of Fe_3O_4@CaAl@Lamivudine.

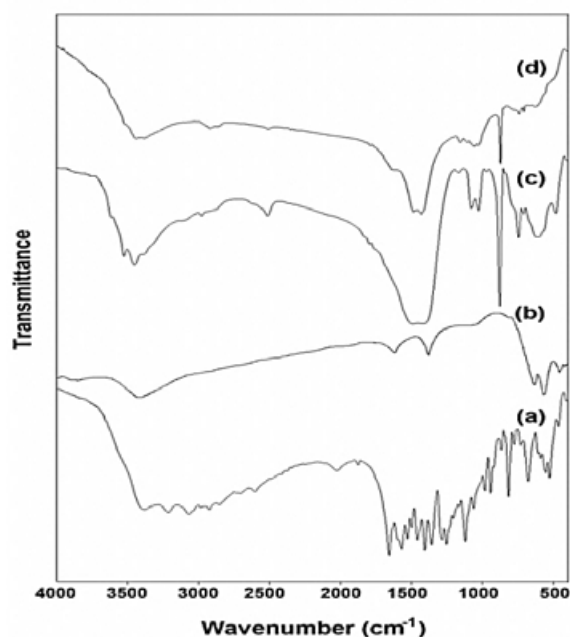Fig. 3. FT-IR Spectra of a) Lamivudine, b) Fe_3O_4, c) Fe_3O_4@CaAl-LDH, and d) Fe_3O_4@CaAl@Lamivudine.

cm^{-1}. Further the peak at 540 cm^{-1} corresponds to the inherent characteristic of the MNPs [20]. The decrease in the intensity of this band in Fe₃O₄@CaAl@Lamivudine spectrum clearly indicates the replacement of CO_3^{2-} anions by Lamivudine molecules. Finally, the FT-IR spectrum of Fe₃O₄@CaAl@Lamivudine shows the characteristic peaks of Fe₃O₄ nanoparticles, CaAl-LDH and Lamivudine which is in agreement with the formation of Fe₃O₄@CaAl@Lamivudine structure (curve d) [21].

Interaction with calf-thymus DNA
UV–vis absorption

In the first step, binding constant measurements were carried out by keeping CT-DNA concentration constant ($5×10^{-5}$ M) during the experiments, Fe₃O₄@LDH@Lamivudine concentration varies from 0 to 13 mg mL^{-1}. The binding constant (K_b) of Fe₃O₄@LDH@Lamivudine with CT-DNA was calculated by UV-Vis absorption spectral analysis and using this equation [22]:

$$\frac{A_0}{A - A_0} = \frac{\varepsilon_G}{\varepsilon_{D-DNA} - \varepsilon_D} + \frac{\varepsilon_G}{\varepsilon_{D-DNA} - \varepsilon_D} \times \frac{1}{K_b[DNA]} \qquad (1)$$

K_b is the binding constant, A and A_0 are the absorbance of nanocomposite-DNA and DNA respectively, ε_D and ε_D-DNA are the molar extinction coefficient of nanocomposite and nanocomposite-DNA complex also respectively [23]. The binding constant, (K_b $4.9×10^3$ M^{-1}) of Fe₃O₄@LDH@Lamivudine with DNA was calculated from ratio of intercept to slop (1/A-A_0 vs. 1/[nanocomposite]). The absorbance was enhanced by increasing the concentration of nanocomposite (Fig. 4). Generally, the hyperchromism occurred due to non-covalent interactions outside the helix

of DNA [24], the absorption band of DNA was observed at 261 nm while the λ_{max} value for Fe₃O₄@LDH@Lamivudine was 268 nm, so we observed 7nm shift to higher wavelengths. The moderate red shift (bathochromic effect) was observed due to the interaction of Fe₃O₄@LDH@Lamivudine nanoparticles with CT-DNA. The noticeable shift in UV-visible wavelength (red shift ≥15 nm) shows the intercalative binding mode of compound to DNA helix because of the interaction of a DNA π stack with compound, on the other hand, outside binders (groove binders) indicate a minor red shift ($\Delta\lambda \le 8$ nm) [22].

The K_b of Fe₃O₄@LDH@Lamivudine and DNA complex ($4.9×10^3$ M^{-1}) was compared with complex of Lamivudine and DNA ($5±0.3 × 10^4$ M^{-1}), binding constant of nanocomposite is one order lower than it's in complex of Lamivudine and DNA. Recent studies reported that, the interaction of Lamivudine with DNA was groove binding [11], we can conclude that, Fe₃O₄@LDH@Lamivudine was created a complex with DNA by groove binding.

Fluorescence emission spectroscopy

The fluorescence Spectroscopy is the most common and reliable techniques that use to investigate the interaction between DNA-compounds and specifies the binding modes [25]. Some compounds show fluorescence properties, due to the special organic functional groups in their structures containing alicyclic carbonyl or aliphatic structures or double-bond conjugated structures. These aromatic groups show low levels of energy in π-π* transition level [22]. Other compounds don't show any fluorescence properties and we have to use some special kind of dyes as the probe [26]. Ethidium bromide (EB) is a fluorophore
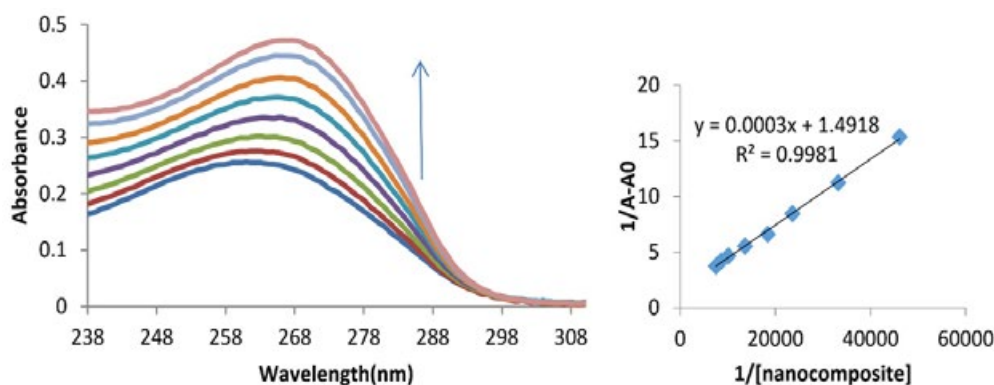

Fig. 4. Absorption spectra of CT-DNA ($5×10^{-5}$ M) in the presence of different concentrations of Fe₃O₄@CaAl LDH@Lamivudine from 0 to $13.0 × 10^{-3}$ g mL^{-1}, at pH=7.4 and room temperature.

that bind to DNA as an intercalative agent. Increasing The fluorescence of EB in the presence of DNA, because of its well-appointed intercalation between the DNA and base pairs [27]. The other intercalative agent is Methylene Blue (MB), this probe has an important application in fluorescence spectroscopy. The intercalation of MB between two near base pairs need unstacking of the base pairs making the binding pocket, and unwrapping the helix of DNA [28]. The most commonly used groove binding agents is Hoechst. This molecule chooses to bind to A-T rich regions of double strand DNA and interact with DNA as a minor groove binding agent. After binding to DNA, Hoechst will withstand an approximately 30-fold enhancement in fluorescence [29]. In this study, we focused on two important probes in fluorescence (MB and Hoechst 33258), to determine the interaction of Fe₃O₄@LDH@Lamivudine with DNA, is associated with which kind of binding modes. Competitive fluorescence studies were carried out by using MB ($5×10^{-6}$ M) as an intercalating agent, shown in Fig. 5. The DNA concentration was kept constant, while increasing the concentration of Fe₃O₄@LDH@Lamivudine, if compound was an intercalative one, it has to replace MB and decreasing fluorescence spectroscopy [30], while there weren't observed any changes or decrement in fluorescence intensity. In the next experiment, Hoechst 33258 ($5×10^{-6}$ M) was used to assure that, Fe₃O₄@LDH@Lamivudine interact with CT-DNA by groove binding mood (Fig. 5b). By increasing the amount of Fe₃O₄@LDH@Lamivudine (0 to 400 μg mL^{-1}), excitation was observed at 412 nm and the intensity of fluorescence was decreased and fill the gap between the spectra of Hoechst and DNA Hoechst. This quenching was occurred due to the replacement of

Hoechst by compound and forming minor groove binding with DNA [31].

Quenching can occur by various mechanisms, which are generally classified as static and dynamic quenching [32]. Commonly, dynamic and static quenching can be diagnosed by their diver's affiliation on temperature and excited-state lifetime [32, 33]. The K_{sv} value (the quenching constant of stern-volmer) was calculated by stern-volmer (Eq. 2):

$$\frac{F_0}{F} = 1 + K_q \tau_0 [Q] = 1 + K_{sv}[Q] \tag{2}$$

In here F_0 and F respectively indicate the fluorescence intensities in the absence and presence of DNA [34]. K_q is the fluorophore quenching rate constant [35], the lifetime of the fluorophore in the absence of a quencher ($\tau_0 = 10^{-8}$), K_{sv} is quenching constant and [Q] is the concentration of compound [36, 37], which here is Fe₃O₄@LDH@Lamivudine. This experiment was carried out in three different temperatures; 288, 298 and 310 K. The K_{sv} decrease from $2.69×10^3$ M^{-1} to $1.25×10^3$ M^{-1} by increasing the temperature, this evidence indicates that the quenching mechanism of nanocomposite with CT-DNA involves static quenching, because K_{sv} decrease with increasing of temperature.

The binding constant (K_b) and the stoichiometry of binding (n) [38], for the formation of new complex between Fe₃O₄@LDH@Lamivudine and DNA were calculated using Eq. 3 :

$$\log \frac{F_0 - F}{F} = \log K_b + n \log [Q] \tag{3}$$

In here, F_0 and F are the intensities of fluorescence's fluorophore in the absence and presence of various amount of CT-DNA [39, 40], n is the number of equivalent binding sites, that
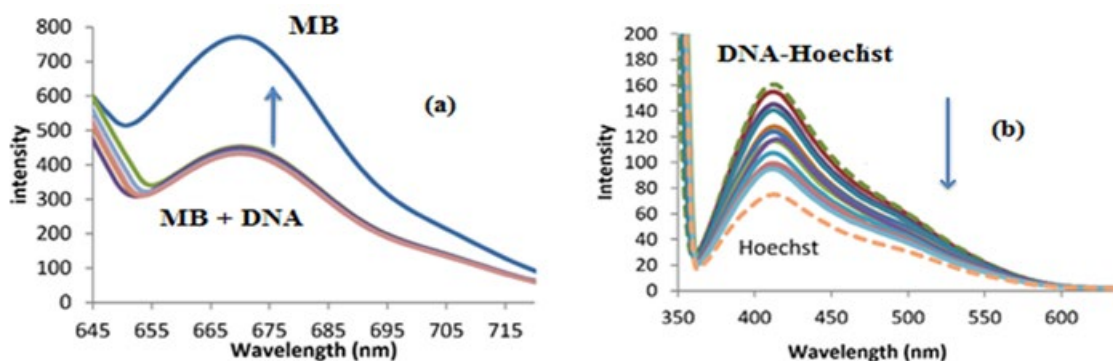

Fig. 5. Competitive fluorescence studies with a) MB, C [MB] = $5.0×10^{-6}$ M, C[CT-DNA] = $2.9×10^{-4}$ M and C [Fe₃O₄@CaAl LDH@ Lamivudine] = 0 to $4×10^{-4}$ g mL^{-1} at pH=7.4 and 310 K, b) Hoechst 33258, C [Hoechst]=$5.0×10^{-6}$ M, C[CT-DNA] = $2.9×10^{-4}$ M and C [Fe₃O₄@CaAl LDH@ Lamivudine] = 0 to $4×10^{-4}$ g mL^{-1} at pH=7.4.

can be determined by the slope based on the Eq.3. The corresponding results at various temperatures (288, 298 and 310 K) are summarized in Table 1. The K_b value at 298 K was 6.43×10^3 L mol^{-1}, which corresponding considerably with K_b (4.9×10^3 L mol^{-1}) that was obtained from the UV-visible technique.

Thermodynamic studies

In order to illustrate the interaction of Fe₃O₄@ LDH@Lamivudine with DNA, the thermodynamic parameters were estimated [41]. The binding force of Fe₃O₄@LDH@Lamivudine with CT-DNA was calculated by K_b. The plot of log K_b versus 1/T (Fig. 6) helped us to compute the enthalpy (ΔH), entropy (ΔS) (Eq. 4) and free energy (ΔG) changes by Eq. 5 [31, 42].

$$\ln Kb = \frac{-\Delta H}{RT} - \frac{\Delta S}{R} \tag{4}$$

$$\Delta G = \Delta H - T\Delta S \tag{5}$$

Which K_b is the binding constant at three different temperatures (288, 298 and 310 K) and R is the gas constant (8.314 J mol^{-1} K^{-1}). Table 1, also display the amount of ΔH, ΔS and ΔG. According to obtained results $\Delta H < 0$ and $\Delta S < 0$, this results indicated that the interaction between DNA and nanocomposite is hydrogen bond and Vander-Waals force [31], and the negative amount of ΔG indicated the spontaneous interaction between nanocomposite and DNA [43].

DNA viscosity experiment

Binding of Compounds to DNA can cause various changes in the length of DNA helix, intercalating binding mode typically increase the length of DNA so a significant change in viscosity measurements will occur [44], increasing the viscosity of DNA is due to compound's intercalation binding with DNA that causes the separation of base pairs in DNA molecules [45]. Groove binding and electrostatic agents don't make significant changes in the viscosity and length of DNA [32]. The changes in the length of DNA were evaluated, by the values of relative specific viscosity $(\eta/\eta_0)^{1/3}$ that were plotted against r (r = [compound]/[DNA]) [46]. The viscosity of the samples (η), the relative specific viscosity $(\eta/\eta_0)^{1/3}$, which η_0 and η are the specific viscosity contributions of CT-DNA in the absence and in the presence of the compound [47, 48]. In this study the concentration of DNA keeps constant (5×10^{-5} M) while varying the concentration of compound (0 to 1 M), by increasing the amount of compound, no change in viscosity was observed (Fig. 7), and the binding mode was described as groove binding [46].

Circular dichroism spectroscopy

CD spectroscopy is a beneficial instrument to recognize alterations in CT-DNA [49]. Morphology changes during the drug–DNA intercalations, since the positive band along with base stacking

Table 1. Binding constants (K_b), number of binding sites (n), and relative thermodynamic parameters for the binding of Fe₃O₄@CaAl LDH@ Lamivudine to CT-DNA.

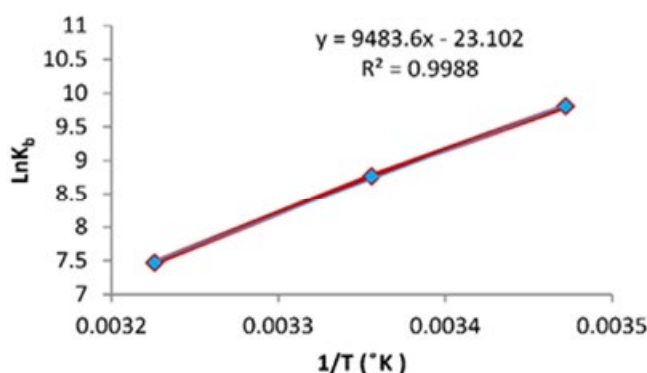| T(°K)	k_{sv}	k_q	K_b	k_d	n	ΔG	ΔH	ΔS
288	2.69×10^3	2.69×10^{11}	1.81×10^4	5.53×10^{-5}	1.29	-23.47	-	-
298	2.07×10^3	2.07×10^{11}	6.43×10^3	1.55×10^{-4}	1.19	-21.72	-78.84	-192.07
310	1.25×10^3	1.25×10^{11}	1.75×10^3	0.57×10^{-3}	1.03	-19.24	-	-

Fig. 6. Van't Hoff plot for the interaction of Fe₃O₄@CaAl-LDH@Lamivudine with CT-DNA at pH=7.4.
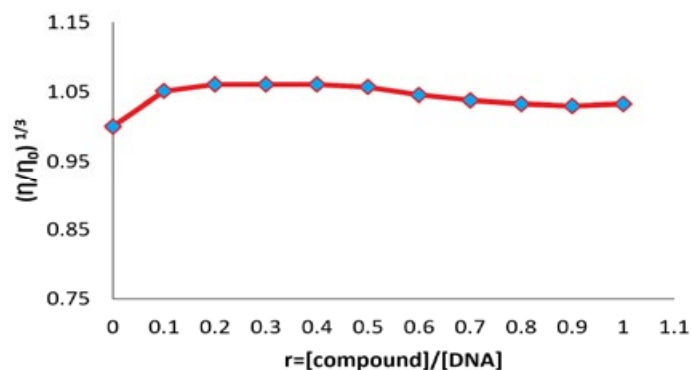
Fig. 7. Viscosity measurements of CT-DNA solution ([CT-DNA] = 5×10^{-5} M, pH = 7.4) in the presence of different amount of Fe$_3$O$_4$@ CaAl LDH@Lamivudine at 298 K.
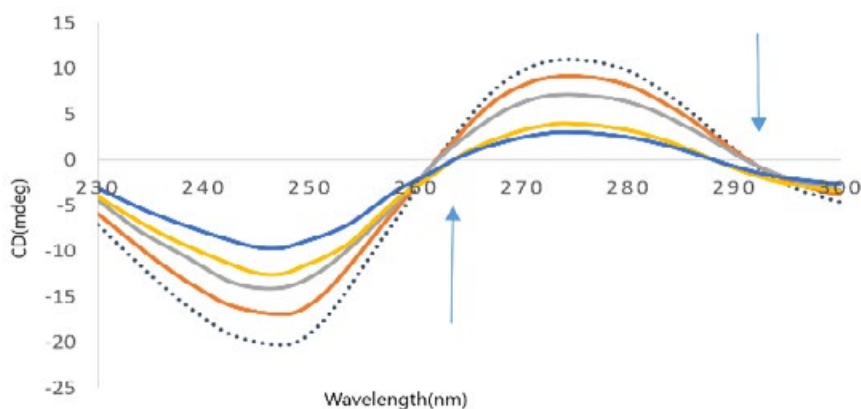
Fig. 8. CD spectra of CT-DNA (5×10^{-6} M) in the absence and presence of Fe$_3$O$_4$@CaAl LDH@Lamivudine (0 – 20 µg mL^{-1}) at room temperature.

(273 nm) and the negative one owing to right-handed helicity (246 nm) are entirely sensitive to the interaction mode of DNA with small molecules [46, 50]. intercalation interaction between drug and DNA cause an enhancement in the intensities of both bands owing to potent base stacking interactions and permanent DNA conformations (right-handed B conformation of CT-DNA), whilst simple groove binding and electrostatic interactions with compounds represent less of a disturbance or no perturbation whatever on the base stacking and helicity bands [51, 52]. By increasing the concentration of the Fe$_3$O$_4$@LDH@Lamivudine (Fig. 8), both positive and negative bands show little changes, which imply a non-intercalative mode between DNA and Fe$_3$O$_4$@LDH@Lamivudine. So in refer to the evidence we can conclude that, the new complex was formed by interaction of nanocomposite and CT-DNA is mainly by groove binding [32, 52].

CONCLUSION

In this study, Fe$_3$O$_4$@LDH@Lamivudine was synthesized and then characterized by TEM, XRD and FT-IR spectroscopy, afterward the interaction of these nanoparticles with CT-DNA has been investigated by fluorescence spectroscopy, Uv-visible spectroscopy, viscosity, circular dichroism (CD). The absorbance of UV-visible spectroscopy was increased by adding the Fe$_3$O$_4$@LDH@Lamivudine, which indicated hyperchromism with the binding constant of (4.9×10^3 M^{-1}). According to obtained results, fluorescence spectroscopy illustrated that the nanocomposite was quenched the substantial fluorescence intensity of CT-DNA through a static quenching procedure. Furthermore, the values of ΔH, ΔS and ΔG were negative, which indicated hydrogen bonding and vander-waals force. Moreover, the viscosity measurements were applied and the results showed that, by enhancing the amount of the nanocomposite, no changes were

observed. The changes which were observed in the CD spectra, display confirmation of the right-handed B form of CT-DNA and suggested the interaction between the nanocomposite and CT-DNA. These experimental results illustrated groove binding interaction of Fe_3O_4@LDH@Lamivudine to CT-DNA.

ACKNOWLEDGMENT

CONFLICT OF INTEREST

The authors declare that there is no conflict of interests regarding the publication of this manuscript.

REFERENCES

[1] I. Haq, Thermodynamics of drug-DNA interactions, Arch. Biochem. Biophys., 403, 1 (2002).

[2] N. Ghinea, M. Little, W. Lipworth, Access to High Cost Cancer Medicines Through the Lens of an Australian Senate Inquiry-Defining the "Goods" at Stake, J. Bioethic. Inq., 14, 401 (2017).

[3] L. Xu, Y.-X. Hu, Y.-C. Li, L. Zhang, H.-X. Ai, Y.-F. Liu, H.-S. Liu, In vitro DNA binding studies of lenalidomide using spectroscopic in combination with molecular docking techniques, J. Mol. Struct., 1154, 9 (2018).

[4] J.B. Mamani, L.F. Gamarra, G.E.d.S. Brito, Synthesis and characterization of Fe_3O_4 nanoparticles with perspectives in biomedical applications, Mater. Res., 17, 542 (2014).

[5] M. Oroujeni, B. Kaboudin, W. Xia, P. Jönsson, D.A. Ossipov, Conjugation of cyclodextrin to magnetic Fe_3O_4 nanoparticles via polydopamine coating for drug delivery, Prog. org. coat., 114, 154 (2018).

[6] G. Choi, T.-H. Kim, J.-M. Oh, J.-H. Choy, Emerging nanomaterials with advanced drug delivery functions; focused on methotrexate delivery, Chem. Rev., 359, 32 (2018).

[7] S. Senapati, R. Shukla, A.K. Mahanta, D. Rana, P. Maiti, Y.B. Tripathi, Engineered Cellular Uptake and Controlled Drug Delivery Using Two Dimensional Nanoparticle and Polymer for Cancer Treatment, Mol. Pharm., (2018).

[8] T.K. Sau, A. Biswas, P. Ray, S. Thota, D.C. Crans, Metal Nanoparticles in Nanomedicine: Advantages and Scope, Metal Nanoparticles: Synthesis, Appl. Pharm. Sci., 155 (2018).

[9] J. Warren Beach, Chemotherapeutic agents for human immunodeficiency virus infection: mechanism of action, pharmacokinetics, metabolism, and adverse reactions, Clinical Therapeutics, 20, 2 (1998).

[10] O. World Health, Consolidated guidelines on the use of antiretroviral drugs for treating and preventing HIV infection: recommendations for a public health approach, W. H. O., 2016.

[11] N. Shahabadi, M. Maghsudi, M. Mahdavi, M. Pourfoulad, Interaction of calf thymus DNA with the antiviral drug lamivudine, DNA cell .biol., 31, 122 (2012).

[12] N. Shahabadi, M. Falsafi, F. Feizi, R. Khodarahmi, Functionalization of γ-Fe_2O_3@SiO_2 nanoparticles using the antiviral drug zidovudine: synthesis, characterization, in vitro cytotoxicity and DNA interaction studies, RSC Adv., 6, 73605 (2016).

[13] N. Shahabadi, M. Razlansari, Exploring the interaction of nanocomposite composed of Fe_3O_4, CaAl layered double hydroxide and lamivudine drug with Human serum albumin (HSA): Spectroscopic studies, J. Nanoanalysis, 5, 107 (2018).

[14] A. Özel, B. Barut, Ü. Demirbaş, Z. Biyiklioglu, Investigation of DNA binding, DNA photocleavage, topoisomerase I inhibition and antioxidant activities of water soluble titanium (IV) phthalocyanine compounds, J. Photochem. Photobiol. B: Biology., 157, 32 (2016).

[15] D. Lazić, A. Arsenijević, R. Puchta, Ž.D. Bugarčić, A. Rilak, DNA binding properties, histidine interaction and cytotoxicity studies of water soluble ruthenium (II) terpyridine complexes, Dalton Trans., 45, 4633 (2016).

[16] N. Shahabadi, A. Khorshidi, H. Zhaleh, S. Kashanian, Synthesis, characterization, cytotoxicity and DNA binding studies of Fe_3O_4@SiO_2 nanoparticles coated by an antiviral drug lamivudine, J. Drug. Deliv. Sci. Technol., 46, 55 (2018).

[17] M. Aghazadeh, One-step cathodic electrosynthesis of surface capped Fe_3O_4 ultra-fine nanoparticles from ethanol medium without using coating agent, Mater. Lett., 211, 225 (2018).

[18] S.J. Kiprono, M.W. Ullah, G. Yang, Encapsulation of E. coli in biomimetic and Fe_3O_4-doped hydrogel: structural and viability analyses, Appl. Microbiol. Biotechnol., 102, 933 (2018).

[19] B. Ma, A. Fernandez-Martinez, S. Grangeon, C. Tournassat, N. Findling, S. Carrero, D. Tisserand, S. Bureau, E. Elkaïm, C. Marini, Selenite uptake by CaAl LDH: a description of intercalated anion coordination geometries, Environ. Sci. Technol., 52, 1624 (2018).

[20] M.P. Bernardo, C. Ribeiro, [Mg-Al]-LDH and [Zn-Al]-LDH as Matrices for Removal of High Loadings of Phosphate, Mater. Res, 21 (2018).

[21] A.K. Jena, A.K. Nayak, A. De, D. Mitra, A. Samanta, Development of lamivudine containing multiple emulsions stabilized by gum odina, J. Pharm. Sci., 4, 71 (2018).

[22] M. Sirajuddin, S. Ali, A. Badshah, Drug-DNA interactions and their study by UV-Visible, fluorescence spectroscopies and cyclic voltametry, J. Photochem. Photobiol., 124, 1 (2013).

[23] M. Parveen, F. Ahmad, A.M. Malla, M.S. Khan, S.U. Rehman, M. Tabish, M.R. Silva, P.S.P. Silva, Structure elucidation and DNA binding specificity of natural compounds from Cassia siamea leaves: A biophysical approach, J. Photochem. Photobiol., 159, 218 (2016).

[24] B.M. Baker, J. Vanderkool, N.R. Kallenbach, Base stacking in a fluorescent dinucleoside monophosphate: εApεA, Biopolymers, 17, 1361 (1978).

[25] M.P. Grant, Synthesis and analysis of platinum (II) sequence selective complexes, (2011).

[26] X. Wen, Q. Wang, Z. Fan, Active fluorescent probe based on aggregation-induced emission for intracellular bioimaging of Zn^{2+} and tracking of interactions with single-stranded DNA, Anal. Chim. Acta., (2018).

[27] M.R. Gill, J.A. Thomas, Targeting cellular DNA with Luminescent Ruthenium (II) Polypyridyl Complexes, Ruthenium Complexes, Photochem. Biomed. Appl., 221

(2017).

[28] L. Cui, M. Lu, Y. Li, B. Tang, C.-y. Zhang, A reusable ratiometric electrochemical biosensor on the basis of the binding of methylene blue to DNA with alternating AT base sequence for sensitive detection of adenosine, Biosens. Bioelectron., 102, 87 (2018).

[29] K.S. Saini, R. Ashraf, D. Mandalapu, S. Das, M.Q. Siddiqui, S. Dwivedi, J. Sarkar, V.L. Sharma, R. Konwar, New orally active DNA minor groove binding small molecule CT-1 acts against breast cancer by targeting tumor DNA damage leading to p53-dependent apoptosis, Mol. Carcinog., 56, 1266 (2017).

[30] M. Gholivand, H. Peyman, K. Gholivand, H. Roshanfekr, A.A. Taherpour, R. Yaghobi, Theoretical and Instrumental Studies of the Competitive Interaction Between Aromatic α-Aminobisphosphonates with DNA Using Binding Probes, Appl. biochem. biotechn., 182, 925 (2017).

[31] T. Sarwar, H.M. Ishqi, S.U. Rehman, M.A. Husain, Y. Rahman, M. Tabish, Caffeic acid binds to the minor groove of calf thymus DNA: A multi-spectroscopic, thermodynamics and molecular modelling study, Int. J. Biol Macromol., 98, 319 (2017).

[32] Y. Sha, X. Chen, B. Niu, Q. Chen, The interaction mode of groove binding between quercetin and calf thymus DNA based on spectrometry and simulation, Chem. Biodivers., (2017).

[33] D. İnci, R. Aydın, Ö. Vatan, Y. Zorlu, N. Çinkılıç, New binary copper (II) complexes containing intercalating ligands: DNA interactions, an unusual static quenching mechanism of BSA and cytotoxic activities, J. Biomol. Struct. Dyn., 1 (2017).

[34] A. Usman, M. Ahmad, Binding of Bisphenol-F, a bisphenol analogue, to calf thymus DNA by multi-spectroscopic and molecular docking studies, Chemosphere, 181, 536 (2017).

[35] C.A. Lelis, E.A. Hudson, G.M.D. Ferreira, G.M.D. Ferreira, L.H.M. da Silva, M.d.C.H. da Silva, M.S. Pinto, A.C. dos Santos Pires, Binding thermodynamics of synthetic dye Allura Red with bovine serum albumin, Food chem., 217, 52 (2017).

[36] N. Shahabadi, B. Bazvandi, A. Taherpour, Synthesis, structural determination and HSA interaction studies of a new water-soluble Cu (II) complex derived from 1, 10-phenanthroline and ranitidine drug, J. Coord. Chem., 70, 3186 (2017).

[37] N. Shahabadi, S. Fatahi, M. Maghsudi, Synthesis of a new Pt (II) complex containing valganciclovir drug and calf thymus DNA interaction study using multispectroscopic methods, J. Coord. Chem., 1 (2018).

[38] N. Shahabadi, M. Falsafi, M. Maghsudi, DNA-binding study of anticancer drug cytarabine by spectroscopic and molecular docking techniques, Nucleosides Nucleotides Nucleic Acids., 36, 49(2017).

[39] P. Jaividhya, M. Ganeshpandian, R. Dhivya, M.A. Akbarsha, M. Palaniandavar, Fluorescent mixed ligand copper (II) complexes of anthracene-appended Schiff bases: studies on DNA binding, nuclease activity and cytotoxicity, Dalton Trans., 44, 11997 (2015).

[40] C. Uvarani, K. Arumugasamy, K. Chandraprakash, M. Sankaran, A. Ata, P.S. Mohan, A New DNA-Intercalative Cytotoxic Allylic Xanthone from Swertia corymbosa, Chem. Biodivers., 12, 358 (2015).

[41] F. Fathi, H. Mohammadzadeh-Aghdash, Y. Sohrabi, P. Dehghan, J.E.N. Dolatabadi, Kinetic and thermodynamic studies of bovine serum albumin interaction with ascorbyl palmitate and ascorbyl stearate food additives using surface plasmon resonance, Food chem., 246, 228 (2018).

[42] Q. Gan, Y. Qi, Y. Xiong, Y. Fu, X. Le, Two New Mononuclear Copper (II)-Dipeptide Complexes of 2-(2′-Pyridyl) Benzoxazole: DNA Interaction, Antioxidation and in Vitro Cytotoxicity Studies, J. Fluoresc., 27, 701 (2017).

[43] B. Sikarwar, V.V. Singh, P.K. Sharma, A. Kumar, D. Thavaselvam, M. Boopathi, B. Singh, Y.K. Jaiswal, DNA-probe-target interaction based detection of Brucella melitensis by using surface plasmon resonance, Biosens. Bioelectron., 87, 964 (2017).

[44] Q. Guo, Z. Zhang, Y. Song, S. Liu, W. Gao, H. Qiao, L. Guo, J. Wang, Investigation on interaction of DNA and several cationic surfactants with different head groups by spectroscopy, gel electrophoresis and viscosity technologies, Chemosphere, 168, 599 (2017).

[45] Z. Adiguzel, S. Ozalp-Yaman, G. Celik, S. Salem, T. Bagci-Onder, F. Senbabaoglu, Y. Cetin, C. Acilan, A platinum blue complex exerts its cytotoxic activity via DNA damage and induces apoptosis in cancer cells, Chem. Biol. Drug. Des., 90, 210 (2017).

[46] S. Pawar, R. Tandel, R. Kunabevu, J. Seetharamappa, Spectroscopic and computational approaches to unravel the mode of binding between a isoflavone, biochanin-A and calf thymus DNA, J. Biomol. Struct. Dyn., 1 (2018).

[47] N. Shakibapour, F. Dehghani Sani, S. Beigoli, H. Sadeghian, J. Chamani, Multi-spectroscopic and molecular modeling studies to reveal the interaction between propyl acridone and calf thymus DNA in the presence of histone H1: Binary and ternary approaches, J. Biomol. Struct. Dyn., 1 (2018).

[48] M. Dehkhodaei, M. Sahihi, H.A. Rudbari, F. Momenbeik, DNA and HSA interaction of Vanadium (IV), Copper (II), and Zinc (II) complexes derived from an asymmetric bidentate Schiff-base ligand: multi spectroscopic, viscosity measurements, molecular docking, and ONIOM studies, JBIC J. Biol. Inorg. Chem., 23, 181 (2018).

[49] M.S. Ali, M.A. Farah, H.A. Al-Lohedan, K.M. Al-Anazi, Comprehensive exploration of the anticancer activities of procaine and its binding with calf thymus DNA: a multi spectroscopic and molecular modelling study, RSC Adv., 8, 9083 (2018).

[50] E.M. Tuite, B. Nordén, Linear and circular dichroism characterization of thionine binding mode with DNA polynucleotides, Spectrochim. Acta Part A Acta A Mol. Biomol. Spectrosc. 189, 86 (2018).

[51] A.G. Clark, M.N. Naufer, F. Westerlund, P. Lincoln, I. Rouzina, T. Paramanathan, M.C. Williams, Reshaping the energy landscape transforms the mechanism and binding kinetics of DNA threading intercalation, Biochem., (2018).

[52] M. Bordbar, F. Tavoosi, A. Yeganeh-Faal, M.H. Zebarjadian, Interaction study of some macrocyclic inorganic schiff base complexes with calf thymus DNA using spectroscopic and voltammetric methods, J. Mol. Struct., 1152, 128 (2018).